On the Origin of Phase Angle in Warburg Finite Length Diffusion Impedance

V.V. Pototskaya[1], O.I. Gichan[2,*]

[1] Vernadskii Institute of General & Inorganic Chemistry, National Academy of Sciences of Ukraine, Palladina Prosp. 32-34, 03142 Kyiv, Ukraine
[2] Chuiko Institute of Surface Chemistry, National Academy of Sciences of Ukraine, Henerala Naumova Str. 17, 03164 Kyiv 164, Ukraine
[*]E-mail: gichan@isc.gov.ua, gichan@meta.ua

We develop a simple physical model which describes the origin of phase angle of the Warburg finite length diffusion impedance. We show that diffusion results in a phase delay of the surface concentration of species with respect to current. The phase shift between current and concentration is a function of a ration of the Nernst diffusion layer thickness to an oscillating length. The phase angle of the Warburg finite length diffusion impedance has a maximum that does not depend on either the Nernst diffusion layer thickness values or the diffusion coefficient of species. The peculiarities of the phase angle changes at the transition from the Warburg finite length diffusion impedance to electrode impedance are shown. The effects of the Nernst diffusion layer thickness, charge-transfer resistance, diffusion coefficient, double layer capacitance, and electrolyte resistance on the behavior of phase angle are discussed.

1. INTRODUCTION

The basis of theoretical studies on the electrode impedance consists in revealing the nature of processes occurring on electrode/electrolyte interface [1-4]. In 1899, Warburg obtained the impedance of a semi-infinite transport layer attached to a planar electrode [5]. Warburg's result has been extended to the transport layer of a finite thickness. A Nernst diffusion model was taken as a basis of the calculations of Warburg finite length impedance [6] on the assumption that transport is exclusively by diffusion. The diffusion contribution of the impedance was studied for a variety of electrode geometries [7] and using different mathematical approaches [8-11]. The authors of Ref [12] proposed a

theoretical model, which describes the properties of the generalized diffusion impedance of bounded diffusion layers, which have low-frequency dispersion. The authors showed that the boundary conditions do not affect the impedance in the range of frequencies higher than the characteristic frequency, $\omega_d = D/d^2$. At low frequencies, the response of the system is a combination of the bulk and limiting properties of the layer.

Barbero considered a transport in slab between two planar electrodes and showed that the account of displacement current on the electrodes leads to the transport impedance differing from the Warburg result [13-16]. According to the author the theoretical interpretation of Warburg's impedance is still an open problem, and its origin is probably related to the boundary conditions. Similar conclusion was made by Kulikovsky, the author showed that the transport layer impedance depends on the type of the electrode connected to the transport layer [17]. To date, the studies of Warburg finite length diffusion impedance in fuel cells and in electrochemical systems with film electrodes remain topical [18-21]. However, the physical origin of phase angle of Warburg finite length diffusion impedance has not been discussed in detail.

In this paper we develop a physical model which describes the physical origin of phase angle of Warburg finite length diffusion impedance. This model allows us to explain the change of phase angle at the transition from the Warburg finite length impedance to electrode impedance. We investigate the impact of such electrochemical system parameters as the Nernst diffusion layer thickness, charge-transfer resistance, diffusion coefficient, double layer capacitance and electrolyte resistance on the behavior of the phase angle.

2. THEORY

2.1. General expressions for the concentration distribution in the near electrode layer

Suppose only one reaction: $\text{Ox} + n\text{e}^- \rightleftarrows \text{Red}$ proceeds at a flat interface. For redox processes, concentration changes under galvanostatic conditions in the near-electrode layer of thickness d can be determined by solving a system of differential equations for Ox and Red species:

$$\frac{\partial c_{ox}}{\partial t} = D_{ox}\frac{\partial^2 c_{ox}}{\partial x^2} \tag{1}$$

$$\frac{\partial c_{red}}{\partial t} = D_{red}\frac{\partial^2 c_{red}}{\partial x^2} \tag{2}$$

where D_{ox} and D_{red} are the diffusion coefficients of Ox and Red species, and x is the normal distance to the electrode surface, c_{ox}, c_{red} are the concentrations of species. In the presence of a supporting electrolyte, migration can be neglected.

Let us take the following initial and boundary conditions:

$$c_{ox}(x,0) = c_{ox}^0, \ c_{red}(x,0) = c_{red}^0 \tag{3}$$

$$c_{ox}(d,t) = c_{ox}^0, \ c_{red}(d,t) = c_{red}^0 \tag{4}$$

At $x = 0$ and $t > 0$, another boundary condition will be:

$$D_{ox}(\partial c_{ox} / \partial x)_{x=0} + D_{red}(\partial c_{red} / \partial x)_{x=0} = 0 \qquad (5)$$

The current density corresponds to the flux density of the reacting species, i.e.:

$$-D_{ox}(\partial c_{ox} / \partial x)_{x=0} = I / nF \qquad (6)$$

where I is an alternating current density, n is the charge of ions, F is the Faraday's constant.

When the alternating current is defined as $I = \text{Re}\{\tilde{i} \exp(j\omega t)\}$, where $\tilde{i}$ is the oscillation amplitude, the concentration distribution in the near-electrode layer for harmonic processes is as follows:

$$c_{ox}(x,t) = c_{ox}^0 + \text{Re}\{\tilde{c}_{ox} \exp(j\omega t)\} \qquad (7)$$

$$c_{red}(x,t) = c_{red}^0 + \text{Re}\{\tilde{c}_{red} \exp(j\omega t)\} \qquad (8)$$

Then the system of equations (1, 2) with respect to the concentration phasors $\tilde{c}_{ox}$, $\tilde{c}_{red}$ takes on the following form:

$$j\omega \tilde{c}_{ox} = D_{ox} \frac{d^2 \tilde{c}_{ox}}{dx^2} \qquad (9)$$

$$j\omega \tilde{c}_{red} = D_{red} \frac{d^2 \tilde{c}_{red}}{dx^2} \qquad (10)$$

with the boundary conditions:

$$\tilde{c}_{ox}(d) = \tilde{c}_{red}(d) = 0 \qquad (11)$$

$$D_{ox} \frac{d\tilde{c}_{ox}(0)}{dx} = -D_{red} \frac{d\tilde{c}_{red}(0)}{dx} = -\frac{\tilde{i}}{nF} \qquad (12)$$

Simple diffusion of the reactant across a stagnant diffusion layer can be analyzed exactly. The system of differential equations (9, 10) has the solution:

$$\tilde{c}_{ox} = a_1 \exp(\sqrt{j\omega / D_{ox}} \, x) + a_2 \exp(-\sqrt{j\omega / D_{ox}} \, x) \qquad (13)$$

$$\tilde{c}_{red} = b_1 \exp(\sqrt{j\omega / D_{red}} \, x) + b_2 \exp(-\sqrt{j\omega / D_{red}} \, x) \qquad (14)$$

The constants a_1, a_2, b_1, b_2 can be found from the boundary conditions (11-12). The expressions for concentration phasors or harmonic concentration oscillation amplitudes near the electrode surface can be written as:

$$\tilde{c}_{ox} = \frac{\tilde{i}}{nF\sqrt{j\omega D_{ox}}} \frac{\text{sh}[\sqrt{j\omega / D_{ox}}(d - x)]}{\text{ch}[\sqrt{j\omega / D_{ox}} \, d]} \qquad (15)$$

$$\tilde{c}_{red} = -\frac{\tilde{i}}{nF\sqrt{j\omega D_{red}}} \frac{\text{sh}[\sqrt{j\omega / D_{red}}(d - x)]}{\text{ch}[\sqrt{j\omega / D_{red}} \, d]} \qquad (16)$$

The concentration phasors of the oxidized and reduced species on the electrode surface $x = 0$ are defined by the formulas:

$$\tilde{c}_{ox}^s = \frac{\tilde{i}}{nF\sqrt{j\omega D_{ox}}} \frac{\text{sh}[\sqrt{j\omega / D_{ox}} \, d]}{\text{ch}[\sqrt{j\omega / D_{ox}} \, d]} = \frac{\tilde{i}}{nF\sqrt{j\omega D_{ox}}} \text{th}\sqrt{j\omega / D_{ox}} \, d \qquad (17)$$

$$\tilde{c}_{red}^s = -\frac{\tilde{i}}{nF\sqrt{j\omega D_{red}}} \frac{\text{sh}[\sqrt{j\omega / D_{red}} \, d]}{\text{ch}[\sqrt{j\omega / D_{red}} \, d]} = -\frac{\tilde{i}}{nF\sqrt{j\omega D_{red}}} \text{th}\sqrt{j\omega / D_{red}} \, d \qquad (18)$$

2.2. Surface concentration of oxidized and reduced particles under polarization by AC and origin of phase angle

Diffusion results in a phase delay of the surface concentration of species with respect to current. Consider the nature of this process. After substituting (17) into (7) and extracting the real part, we find the surface concentration:

$$c_{ox}^s = c_{ox}^0 + \Delta c_{ox}^s = c_{ox}^0 + \frac{\tilde{i}}{nF}\frac{d}{D_{ox}}\left(\frac{1}{y}\frac{\text{sh }y + \sin y}{(\text{ch }y + \cos y)}\cos \omega t + \frac{1}{y}\frac{\text{sh }y - \sin y}{(\text{ch }y + \cos y)}\sin \omega t\right) \quad (19)$$

with $y = 2d\sqrt{\dfrac{\omega}{2D_{ox}}}$.

After some mathematical calculation, the expression for Δc_{ox}^s can be written as:

$$\Delta c_{ox}^s = \frac{\tilde{i}}{nF}\frac{d}{D_{ox}}r_{ox}\sin(\omega t + \theta_{ox}) \quad (20)$$

where $r_{ox} = \dfrac{\sqrt{2}(\text{sh}^2 y + \sin^2 y)^{1/2}}{y(\text{ch }y + \cos y)}$.

The phase shift θ takes the form:

$$\theta_{ox} = \arcsin\frac{\sin y + \text{sh }y}{\sqrt{2}[\text{sh}^2 y + \sin^2 y]^{1/2}} \quad (21)$$

Similar calculations can be made for the case of c_{red}^s :

$$\Delta c_{red}^s = -\frac{\tilde{i}}{nF}\frac{d}{D_{red}}r_{red}\sin(\omega t + \theta_{red}) \quad (22)$$

$$\theta_{red} = \arcsin\frac{\sin ay + \text{sh}ay}{\sqrt{2}[\text{sh}^2 ay + \sin^2 ay]^{1/2}} \quad (23)$$

with $r_{red} = \dfrac{\sqrt{2}(\text{sh}^2 ay + \sin^2 ay)^{1/2}}{ay(\text{ch }ay + \cos ay)}$, $a = \sqrt{D_{ox}/D_{red}}$.

The phase shift between current and concentration (potential), which changes under the action of this current, will be defined by expressions (21, 23). This is our main result. The phase angle is a function of the ratio of the Nernst diffusion layer thickness d to the oscillation diffusion layer $d_f = \sqrt{D/\omega}$. In the high-frequency range, the following relation is fulfilled, $\theta = 45°$, as for the case of semi-infinite diffusion [21].

3. RESULTS AND DISCUSSION

3.1. Estimation of the Warburg finite length impedance phase angle for Ox species. Effect of diffusion layer thickness

The Warburg finite length diffusion impedance of the system is defined as [3]:

$$Z_W = Z_{ox} + Z_{red} = \frac{RT}{(nF)^2}\left(\frac{\text{th}\sqrt{j\omega/D_{ox}}d}{c_{ox}^0\sqrt{j\omega D_{ox}}} + \frac{\text{th}\sqrt{j\omega/D_{red}}d}{c_{red}^0\sqrt{j\omega D_{red}}}\right) \quad (24)$$

where R is the gas constant, T is the absolute temperature.

The phase angles can be calculated from the formulas:

$$\phi_{ox} = -\text{arctg}[\frac{\text{sh } y - \sin y}{\text{sh } y + \sin y}], \ \phi_{red} = -\text{arctg}[\frac{\text{sh } ay - \sin ay}{\text{sh } ay + \sin ay}] \tag{25}$$

The phase angle $\phi = \arg Z_{ox}$ depends on frequency and increases from zero to the maximum value of $\phi = -46.6°$ ($d/d_f \approx 2.78$), then decreases to $\phi = -45°$ and afterwards is observed to be constant, as with classical Warburg impedance. The maximum phase angle appears in the frequency range at which the transition from the Warburg finite length impedance to the classical Warburg impedance occurs. The maximum value of the phase angle does not depend on either the Nernst diffusion layer thickness d values or the diffusion coefficient of species. On these parameters, the value of frequency corresponding to the maximum of the phase angle depends. With decreasing the Nernst diffusion layer thickness d, the curves of the frequency dependence of the phase angle shift to the right (Figure 1). The position of the maximum value of the phase angle on the Nyquist diagram depends only on frequency and the parameter $\lambda = d/d_f$. At this point, a value of λ is the same for all values of the Nernst diffusion layer thickness, $\lambda \approx 2.78$. Also at this point, the values of imaginary and active components of impedance are the same for all d values. Thus, the boundary conditions for diffusing particles significantly affect the dependence of the phase angle on the frequency.
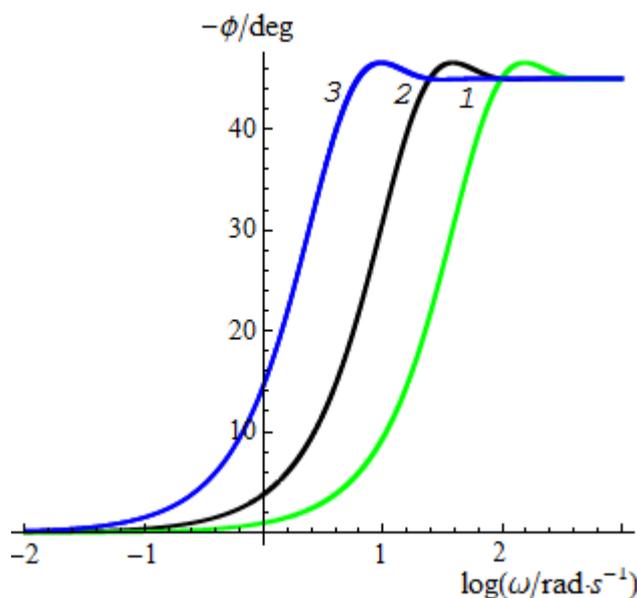

Figure 1. Phase angle of normalized Warburg finite length diffusion impedance for oxidized species, ϕ/deg, as a function of logarithm of frequency, $\log(\omega/\text{rad}\cdot\text{s}^{-1})$, for different values of the Nernst diffusion layer, d/cm, as follows: (1) $5\cdot10^{-4}$; (2) 10^{-3}; (3) $2\cdot10^{-3}$. Here and below, $D_{ox} = 5\cdot10^{-6}\text{cm}^2/s$, T=300 K, n=1.

3.2. Diffusion coefficient effect

The expressions (21, 23) for phase angle θ are obtained for the first time. They provide an alternative explanation for the physical origin of phase angle of Warburg finite length diffusion

impedance. Figure 2 presents the dependence of phase angle θ on frequency for oxidized and reduced species. Phase angle is due to diffusion of particles in a near-electrode layer under application of a harmonic perturbation, $\theta = 90° + \phi$, where ϕ is the phase angle of phase shift at impedance measurement. The phase angle shift depends on diffusion coefficient so it can differ for oxidized and reduced species at given frequency. When diffusion coefficient of reduced species is greater than that of oxidized species, a shift of the curve of the reduced form takes place in the range of high frequencies. This behavior of the phase angle is determined by boundary conditions. For semi-infinite diffusion, the phase angle is independent of frequency [22].
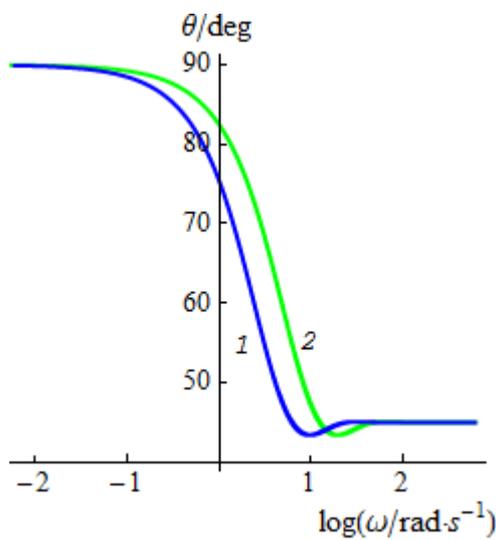
Figure 2. Dependence of phase angle, $\theta / \deg$, for oxidized (1) and reduced species (2) on logarithm of frequency, $\log(\omega / \mathrm{rad} \cdot \mathrm{s}^{-1})$. Here and below, $d = 2 \cdot 10^{-3} \mathrm{cm}$, $D_{red} = 10^{-5} \mathrm{cm}^2 / s$.

3.3. The Faradaic impedance phase angle estimation. Dependence on charge-transfer resistance

The Faradaic impedance describes intrinsic properties of the electrochemical system. In the case of mixed polarization, the overvoltage is due to both concentration polarization and the slowness of the charge transfer stage. The fundamental relationship between current and applied overvoltage is described by the Butler-Volmer equation [23, 24]:

$$I = I_0 \{ \frac{c_{ox}^s}{c_{ox}^0} \exp \frac{\alpha nF}{RT} \eta - \frac{c_{red}^s}{c_{red}^0} \exp[- \frac{(1-\alpha)nF}{RT} \eta] \} \tag{26}$$

Here $\eta = E - E_0$ – overvoltage of the electrode, E_0 – equilibrium potential, I_0 – exchange current, α – the charge transfer coefficient. For the case of $\eta << \frac{RT}{nF}$ we can expand the exponent in a row and limit to a linear term. The Faradaic impedance will be described by the expression [3, 23, 24]:

$$Z_f = R_{ct} + Z_{ox} + Z_{red} \tag{27}$$

where charge - transfer resistance is:

$$R_{ct} = \frac{RT}{nF} \frac{1}{I_0} \qquad (28)$$

Z_{ox}, Z_{red} are determined by expression (24).

We normalized Z_f to the quantity $\sigma_{ox} = \dfrac{RT}{(nF)^2} \dfrac{d}{D_{ox} c_{ox}^0}$ ($\Omega \cdot cm^2$), which is Warburg constant for oxidized species:

$$\tilde{Z}_f = \tilde{R}_{ct} + \frac{1}{y}\left(\frac{\mathrm{sh}\,y + \sin y}{\mathrm{ch}\,y + \cos y} + \gamma\,\frac{\mathrm{sh}\,ay + \cos ay}{\mathrm{ch}\,ay + \cos ay}\right) - j\frac{1}{y}\left(\frac{\mathrm{sh}\,y - \sin y}{\mathrm{ch}\,y + \cos y} + \gamma\,\frac{\mathrm{sh}\,ay - \sin ay}{\mathrm{ch}\,ay + \cos ay}\right) \qquad (29)$$

where

$$\tilde{Z}_f = Z_f \frac{(nF)^2}{RT}\frac{D_{ox}c_{ox}^0}{d}; \quad \tilde{R}_{ct} = R_{ct}\frac{(nF)^2}{RT}\frac{D_{ox}c_{ox}^0}{d}; \quad \gamma = \frac{D_{ox}^{1/2}}{D_{red}^{1/2}}\frac{c_{ox}^{1/2}}{c_{red}^{1/2}} \qquad (30)$$

Phase angle can be written as:

$$\mathrm{tg}\,\phi = -\frac{\mathrm{Im}[\tilde{Z}_{ox} + \tilde{Z}_{red}]}{\tilde{R}_{ct} + \mathrm{Re}[\tilde{Z}_{ox} + \tilde{Z}_{red}]} \qquad (31)$$

Table 1 presents numerical values of some parameters of the electrochemical system in the maximum of phase angle ϕ with variation of the charge - transfer resistance R_{ct}.

Table 1. Numerical values of the parameters in the maximum of the Faradaic impedance phase angle ϕ with variation of the charge transfer resistance R_{ct}

R_{ct} ($\Omega \cdot cm^2$)	$-\phi_{max}$ (deg)	ω_{max} (rad$\cdot$s^{-1})	$Z_f'(\omega_{max})$ ($\Omega \cdot cm^2$)	$-Z_f''(\omega_{max})$ ($\Omega \cdot cm^2$)
0	46.33	18.47	0.18	0.19
0.5	18.94	8.05	0.82	0.28
1	12.14	6.95	1.36	0.29

Figure 3 shows the Faradaic impedance phase angle as a function of frequency for different values of charge - transfer resistance. As the charge - transfer resistance increases, the phase angle maximum shifts to lower frequencies and the magnitude of the maximum decreases. For large values R_{ct} the phase angle tends to zero.

In the calculations, we neglected the resistance of electrolyte and did not take into account the double layer impedance. In this case, the impedance of the model system under consideration is equal to Faradaic impedance $Z = Z_f$. Assuming that the process of double layer charging and Faradaic process can be separated and double layer capacitance C_{dl} is arranged in parallel to Faradaic impedance, interface impedance can be written as:

$$Z_{int} = (1/Z_f + j\omega C_{dl})^{-1} \qquad (32)$$

Total electrode impedance of the cell is a sum of serial resistance R_s and interface impedance Z_{int}:

$$Z = R_s + Z_{int}, \qquad\qquad (33)$$

where R_s is the sum of resistance of electrolyte and external resistance.
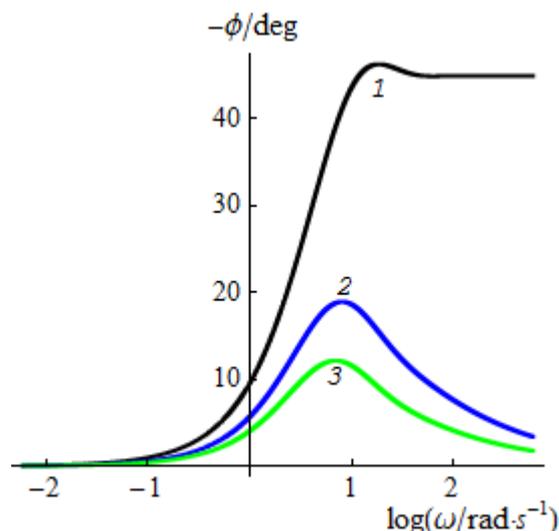
Figure 3. Faradaic impedance phase angle, $\phi / \deg$, as a function of logarithm of frequency, $\log(\omega / \mathrm{rad \cdot s}^{-1})$, for different values of charge - transfer resistance $R_{ct} / \Omega \cdot \mathrm{cm}^2$ as follows: (1) 0; (2) 0.5; (3) 1. Numerical values of used parameters were: $c_{ox}^0 = 5 \cdot 10^{-4}$ mol cm^{-3}, $c_{red}^0 = 10^{-4}$ mol cm^{-3}.
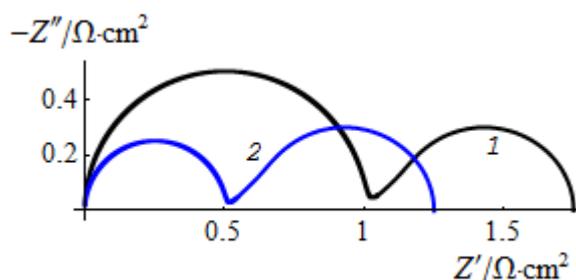
3.4. Interface impedance. Dependence of phase angle on double layer capacitance

The interface impedance phase angle does not depend on double layer capacitance C_{dl} at zero charge - transfer resistance. However, for the case of $R_{ct} > 0$ it depends on the C_{dl} value. At the chosen values of $R_{ct} = 0.5$ $\Omega \cdot \mathrm{cm}^2$ and $R_{ct} = 1$ $\Omega \cdot \mathrm{cm}^2$, the phase angle has a maximum as in the case of Faradaic impedance. In the range of frequencies where Warburg impedance tends to zero, the phase angle starts to rise as quicker as higher a value of R_{ct} is. The phase angle tends to the value of $-\pi / 2$ at high frequencies (Figure 4). In Ref. [25], the electrochemical behavior of a copper sulfide electrode in a sulfate bath containing Cu^{2+} ions was studied. Authors calculated Bode plots in the range of frequencies where Warburg finite length diffusion impedance turns to classic Warburg impedance. The general equation of the Faradaic impedance was the sum of three terms: charge transfer resistance, the impedance corresponding to the diffusion of copper ions in the solution and the impedance corresponding to the diffusion of copper in the solid. In the calculation the authors supposed that at the middle frequencies, the double layer capacitance contribution is negligible. The phase angle of impedance corresponding to the diffusion of copper ions in the solution has similar dependence on frequency as in Figure 4 (curves 2 and 3).
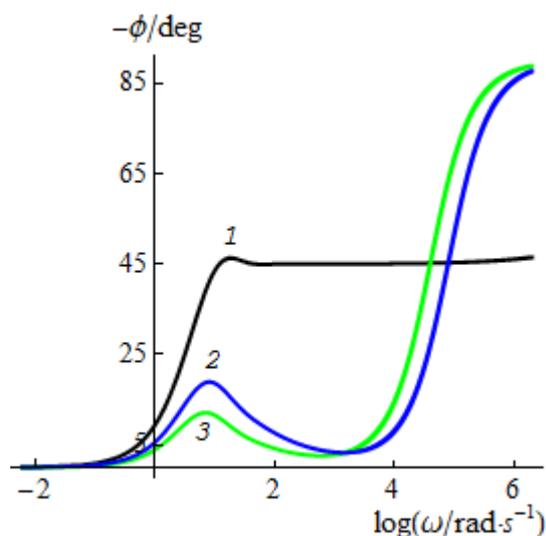
Figure 4. Interface impedance phase angle, $\phi/\deg$, as a function of logarithm of frequency, $\log(\omega/\mathrm{rad}\cdot\mathrm{s}^{-1})$, for different values of charge - transfer resistance $R_{ct}/\Omega\cdot\mathrm{cm}^2$ as in Fig 3. Here and below, $C_{dl} = 2.5\ 10^{-5}$ F cm^{-2}.

Figure 5 shows the complex-plane plots of the interface impedance for different R_{ct} values. The diagram consists of two loops. The left loop corresponds to the charge-transfer impedance. The size of the loop depends on the R_{ct} value. The radius of the semi-circle is equal to $R_{ct}/2$. The size of the right loop does not depend on the R_{ct} value. In Ref. [20], using the fractional modeling of Nernst diffusion, the similar Nyquist plot was obtained.

Figure 5. Nyquist plots of the interface impedance for different values of charge - transfer resistance $R_{ct}/\Omega\cdot\mathrm{cm}^2$ as follows: (1) 1; (2) 0.5.

3.5. Electrode impedance. Dependence of phase angle on electrolyte resistance

Figure 6 presents the dependence of electrode impedance phase angle on frequency for different values of electrolyte resistance at given values of the parameters C_{dl} and R_{ct}.
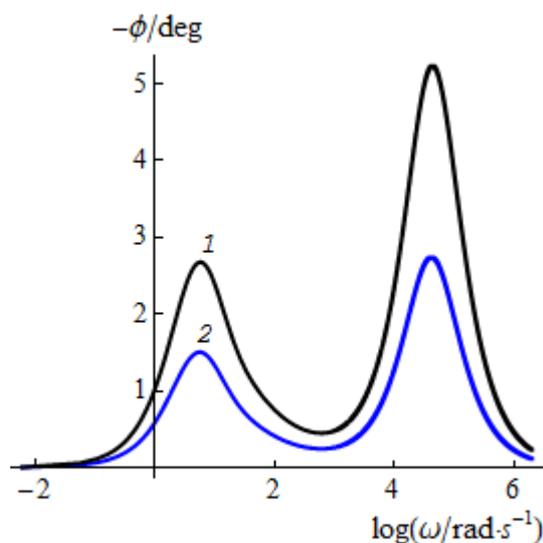
Figure 6. Electrode impedance phase angle, ϕ/deg, as a function of logarithm of frequency, $\log(\omega/\text{rad}\cdot\text{s}^{-1})$, for different values of electrolyte resistance $R_s/\Omega\cdot\text{cm}^2$ as follows: (1) 5; (2) 10. Here, $R_{ct} = 1\ \Omega\cdot\text{cm}^2$.

The phase angle has two maxima; the first peak is in the range of low frequencies and the second one is in the range of high ones, where Warburg impedance is equal to zero. With increasing a value of electrolyte resistance, the both maxima of the phase angle decrease. All numerical calculations were performed on the basis of the mathematical package Mathematica$^{\text{TM}}$ [26].

4. CONCLUSION

Thus, in this paper we demonstrated that the physical origin of phase angle of Warburg finite length diffusion impedance is determined by diffusion. We showed the peculiarities of the phase angle change with a variation of frequency and other parameters of the electrochemical system.

References

1. M. E. Orazem, B. Tribollet, Electrochemical Impedance Spectroscopy, 2nd ed., John Wiley & Sons, (2017) Hoboken.
2. E. Barsoukov and J. R. Macdonald, Editors, Impedance Spectroscopy: Theory, Experiment, and Applications, 2nd ed., Wiley, (2005) New Jersey.
3. A. Lasia, Electrochemical impedance spectroscopy and its applications, Springer Science+Business Media, (2014) New York.
4. D. D. Macdonald, *Electrochim. Acta*, 51 (2006) 1376.
5. E. Warburg, *Ann. Physik und Chemie*, 67 (1899) 493.
6. P. Drossbach and J. Schulz, *Electrochim. Acta*, 9 (1964) 1391.
7. T. Jacobsen and K. West, *Electrochim. Acta*, 40 (1995) 255.
8. D.R. Franceschetti, J.R. Macdonald and R.P. Buck, *J. Electrochem. Soc.*, 136 (1991) 1368.
9. J.-P. Diard, B. Le Gorres and C. Montella, *J. Electroanal. Chem.*, 471 (1999) 126.

10. J.-P. Diard, B. Le Gorres and C. Montella, Handbook of Electrochemical Impedance Spectroscopy. Diffusion impedances, ER@SE/LEPMI, (2017) Hosted by Bio-Logic@www.bio-logic.info.
11. A.A. Moya, *Phys. Chem. Chem. Phys.*, 18 (2016) 3812-6.
12. J. Bisquert, G. Garcia-Belmonte, F. Fabregat-Santiago and P.R. Bueno, *J. Electroanal. Chem.*, 475 (1999) 152.
13. G. Barbero, *Phys. Chem. Chem. Phys.*, 18 (2016) 29537.
14. G. Barbero, I. Lelidis, *Phys. Chem. Chem. Phys.*, 19 (2017) 24934.
15. G. Barbero, *Phys. Chem. Chem. Phys.*, 19 (2017) 32575.
16. I. Lelidis and G. Barbero, *Phys. Rev.*, *E*, 95 (2017) 052604.
17. A. Kulikovsky, *Electrochem. Commun.*, 84 (2017) 28.
18. J.D. Gabano, T. Poinot and B. Huard, *Commun. Nonlinear Sci. Numer. Simul.*, 47 (2017) 164.
19. J. Huang, *Electrochim. Acta,* 281 (2018) 170.
20. A. N. Eddine, B. Huard, J. D. Gabano and T. Poinot, *Commun. Nonlinear Sci. Numer. Simul.*, 59 (2018) 375.
21. M. Schönleber, C. Uhlmann, P. Braun, A. Weber and E. Ivers-Tiffée, *Electrochim. Acta*, 243 (2017) 250.
22. Y. Takemori, T. Kambara, M. Senda and I. Tachi, *J. Phys. Chem.*, 61 (1957) 968.
23. B. B. Damaskin, O. A. Petriy and G. A. Tsirlina, Elektrikhimiya, *Khimiya Kolos S*, (2008) Moskva.
24. C. Gabrielli, in Physical Electrochemistry: Principles, Methods, and Applications, I. Rubinstein, Editor, Marcel Dekker (1995) New York.
25. S. Sanchez, S. Cassaignon, J. Vedel and H. G. Meier, *Electrochim. Acta*, 41 (1996) 1331.
26. S. Wolfram, Mathematica^{TM}, Addison Wesley (1988) Redwood City.